Geomechanics and Engineering, *Vol. 16, No. 3 (2018) 257-271*
DOI: https://doi.org/10.12989/gae.2018.16.3.257

Investigation of influence of homogenization models on stability and dynamic of FGM plates on elastic foundations

Tewfik Mehala[1], Zakaria Belabed[1,2], Abdelouahed Tounsi*[1,3] and O. Anwar Bég[4]

[1]*Material and Hydrology Laboratory, Faculty of Technology, Civil Engineering Department, University of Sidi Bel Abbes, Algeria*
[2]*Department of Technology, Institute of Science and Technology, Center University of Naama, Algeria*
[3]*Department of Civil and Environmental Engineering, King Fahd University of Petroleum & Minerals, 31261 Dhahran, Eastern Province, Saudi Arabia*
[4]*Aeronautical and Mechanical Engineering, University of Salford, Newton Building, G77, The Crescent, Salford, M54WT, England, U.K.*

(Received January 23, 2018, Revised May 14, 2018, Accepted June 12, 2018)

Abstract. In this paper, the effect of the homogenization models on buckling and free vibration is presented for simply supported functionally graded plates (FGM) resting on elastic foundation. The majority of investigations developed in the last decade, explored the Voigt homogenization model to predict the effective proprieties of functionally graded materials at the macroscopic-scale for FGM mechanical behavior. For this reason, various models have been used to derive the effective proprieties of FGMs and simulate thereby their effects on the buckling and free vibration of FGM plates based on comparative studies that may differ in terms of several parameters. The refined plate theory, as used in this paper, is based on dividing the transverse displacement into both bending and shear components. This leads to a reduction in the number of unknowns and governing equations. Furthermore the present formulation utilizes a sinusoidal variation of displacement field across the thickness, and satisfies the stress-free boundary conditions on the upper and lower surfaces of the plate without requiring any shear correction factor. Equations of motion are derived from Hamilton's principle. Analytical solutions for the buckling and free vibration analysis are obtained for simply supported plates. The obtained results are compared with those predicted by other plate theories. This study shows the sensitivity of the obtained results to different homogenization models and that the results generated may vary considerably from one theory to another. Comprehensive visualization of results is provided. The analysis is relevant to aerospace, nuclear, civil and other structures.

Keywords: buckling; vibration; FGM; plate theory; elastic foundation; homogenization models

1. Introduction

Functionally graded materials (FGMs) are a relatively new class of advanced composite materials that are becoming increasingly important on account of their many advantages. This class of materials was discovered by Japanese scientists and designed to prepare thermal barrier materials (Yamanouchi *et al.* 1990, Koizumi 1993, 1997). With rapid developments in modern technology (e.g., nuclear, gas turbine and rocket chamber design), a variety of requirements including enhanced thermal shock resistance, the necessity for high hardness and high toughness in wear-resistant coatings, higher corrosion resistance and longer fatigue life, have accelerated the implementation of functionally graded materials in diverse engineering systems. FGMs are considered as non-conventional composite materials that are microscopically non-homogeneous and with mechanical properties which vary continuously and smoothly through the thickness coordinate. These characteristics eliminate and reduce the influence of stress concentration generally encountered in laminated composites. Moreover, the concept of a typical FGM is based on a mixture of two distinct material phases, generally ceramic and metal by the volume fraction of the constituent materials through the thickness of structural element (Behravan Rad 2012, Ahmed 2014, Behravan Rad 2015, Bousahla *et al.* 2016, El-Haina *et al.* 2017, Behravan Rad *et al.* 2017, Bellifa *et al.* 2017a, Abdelaziz *et al.* 2017, Karami *et al.* 2017 and 2018a, b, c, Shahsavari *et al.* 2018, Attia *et al.* 2018; Fourn *et al.* 2018, Belabed *et al.* 2018). The large-scale utilization of FGMs requires a robust mathematical description of their mechanical proprieties which is needed to represent accurately the response of these materials at the macroscopic level.

Although experimental investigations of FGM plates have been communicated, the benefits of mathematical modeling of functionally graded plates provide a more cost-effective and indeed alternative approach for predict their responses. Models can also be corroborated with experimental data. Theoretical analysis of FGMs has therefore emerged as a substantial body of research examining a wide spectrum of problems. Many studies have been presented on accurate plate theories which combine classical plate theory and shear deformation plate theory to simulate static, buckling and dynamic behaviors of functionally graded plates. Founded on the kinematic field assumptions, these plate theories are developed in accordance with the plate thickness-to-length ratio. The

*Corresponding author, Professor
E-mail: tou_abdel@yahoo.com or
abdelouahed.tounsi@univ-sba.dz

ISSN: 2005-307X (Print), 2092-6219 (Online)

classical plate theory (CPT) neglects shear deformations and therefore it is truly accurate only for thin plates. CPT has been deployed for buckling analysis of FGM plates by various investigators including Feldman and Aboudi (1997), Mahdavian (2009), and Mohammadi *et al.* (2010). However CPT *over-predicts* the natural frequencies and critical buckling loads of thick plates. This limitation can be avoided by introducing the effects of *transverse shear deformation*. First-order shear deformation theory (FSDT) (Reissner 1945, Mindlin 1951, Al-Basyouni *et al.* 2015, Bouderba *et al.* 2016, Youcef *et al.* 2018) considers transverse shear deformation; this theory recommends a shear correction factor in order to satisfy the zero transverse shear stress boundary conditions at the top and bottom of the plate. Indeed in CPT the displacements, strains and stresses fields are assumed to obey a linear distribution through the thickness of plate. However this linear behavior does not describe correctly the variation of these variables. This shortcoming has mobilized interest in developing a more accurate approach which better represent the stress and strain fields through the thickness of plate. To achieve improved accuracy, various higher-order shear deformation plate theories (HSDTs) have been developed and implemented in recent years to analyze the responses of thick functionally graded plates in various loading scenarios. The majority of higher-order shear deformation plate theories incorporate a *nonlinear* distribution to represent the displacement field. These theories feature a different number of unknowns to each other. For example the HSDT theory of Nelson and Lorch (1974) features *nine* unknowns, that of Lo *et al.* (1977) has *eleven* unknowns, the model of Reddy (1984) uses *five* unknowns, Bounouara *et al.* (2016) also employ *five* unknowns. Other HSDT models include those of Kant and Pandya (1988) with *seven* unknowns, Kant and Khare (1997) with *nine* unknowns and Talha and Singh (2010) with *eleven* unknowns. A good review of these theories for the analysis of functionally graded plates is available in Swaminathan *et al.* (2015).

In addition, the higher-order shear deformation plate theories are capable of much better representation of the distribution of displacement, strains and stress through the thickness of plate compared with classical plate theory and First-order shear deformation theory. However the resulting equations of motion are much more complicated since they invariably generate a host of unknowns. Recently, an accurate refined higher order shear deformation theory (RHSDT) has however been developed which is relatively simple to use and simultaneously retains important physical characteristics. Applications of the RHSDT approach (with only four unknowns) to various problems in bending, buckling and dynamics of FGM plates are addressed in the papers of Benyoucef *et al.*(2010), Bouderba *et al.*(2013), Tounsi *et al.*(2013), Zidi *et al.* (2014), Ait Yahia *et al.* (2015), Barati *et al.* Shahverdi (2016) and Younsi *et al.* (2018). The displacement field is chosen based on a *nonlinear* variation of in-plane and transverse displacements through the thickness. Partitioning the transverse displacement into the bending and shear components leads to a reduction in the number of unknowns, and consequently, makes these theories much more amenable to mathematical implementation. Recently, Wang and Zu (2017a) studied the nonlinear steady-state responses of longitudinally traveling FGM plates immersed in liquid for the first time. Wang and Zu (2017b) investigated the dynamic thermoelastic response of rectangular FGM plates with longitudinal velocity. Using Rayleigh-Ritz method, Wang and Zu (2017c) studied analytically the vibration of a longitudinally moving rectangular plate submersed in an infinite liquid domain.

An additional factor which can be observed in many research papers dealing with functionally graded plates is the relative sparseness of studies considering the effect of micromechanical models on macroscopic behaviors. In most investigations the *Voigt model* is considered as principal homogenization model which predicts the effective mechanical properties as being Young's modulus and Poisson's ratio, for homogenized functionally graded plates.

Several micromechanical models have been examined and tested to estimate the effective properties of functionally graded materials, based on *volume fraction distribution* by Zuiker(1995) who has elaborated on the important limitation on structural mechanics property variation. Reiter and Dvorak (1997) presented a numerical simulation based on Mori-Tanaka method to predict the elastic responses for several functionally graded microstructures under different traction and mixed boundary conditions. An extension of this work for thermomechanical loading was subsequently communicated by Reiter and Dvorak (1998). Gasik (1998) summarized the important homogenization models used for composites and functionally graded materials and discussed the effect of the derived thermo-mechanical properties of these models on elastic and plastic thermal stress analysis of FGMs.

Cho and Ha (2001) compared results obtained by two classical averaging approaches for predicting the Young's modulus and the thermal expansion coefficient for functionally graded materials, namely the Wakashima-Tsukamoto linear modified mixture rule and the finite-element discretization approach utilizing rectangular cells. Schmauder and Weber (2001) presented numerical results for homogenization modeling of functionally graded materials also benchmarking their solutions with experimental findings. Paulino *et al.* (2003) elucidated on a range of micro-mechanics models for predicting the elastic effective proprieties of FGMs and their failure behavior. Yin *et al.* (2004) obtained novel results via a micromechanical model for the effective elastic behavior of functionally graded materials with particle interactions based on Eshelby's equivalent inclusion method.

The above articles provide a perspective of the various homogenization models deployed to derive the effective elastic proprieties of functionally graded materials and gain knowledge about engineering properties and structural behaviors. Moreover, these studies provide an insight into the behavior of such materials at the microscopic scale; it is also necessary from an engineering perspective to show the influence of microscopic behavior on global structural (macroscopic) response. Several comprehensive studies are available for providing a good methodology with regard to predicting the effect of homogenization models on functionally graded plate responses at the macroscopic scale. Vel and Batra (2004) used the Mori-Tanaka and self-consistent schemes to obtain three-dimensional exact

solutions for vibration response of functionally graded rectangular plates, although they did not deliberate to any great extent on the physical implications of their solutions. Ferreira *et al.* (2005) estimated the effective proprieties by the rule of mixtures and the Mori-Tanaka scheme to analyze static deformations of a simply supported functionally graded plate. Ferreira *et al.* (2006) later presented solutions for the free vibration of functionally graded plates based on third-order shear deformation plate theories. Shen *et al.* (2012) assessed the viability of both the Voigt and Mori-Tanaka models for vibration analysis of functionally graded plates. Belabed *et al.* (2014) presented an efficient and simple higher order shear plate theory, considering three distribution material models (i.e., the power law distribution, the exponential distributions, and the Mori-Tanaka scheme) to derive elastic proprieties for both the static and dynamic cases. Recently, Akbarzadeh *et al.* (2015) explored the relative performance of a diverse range of homogenization models (i.e., Voigt, Reuss, Hashin-Shtrikman bounds, LRVE and self-consistent model)and their effect on the static and dynamic stress fields, critical buckling loads, and fundamental frequency of functionally graded plate resting on a Pasternak elastic foundation.

In this study, the effect of homogenization models on buckling and free vibration is investigated for thick functionally graded plates resting on elastic foundations, to evaluate the effective elastic proprieties such as Young's modules, Poisson's ratio and mass density. A range of explicit homogenization models are utilized such as the Voigt, Reuss, Hashin-Shtrikman bounds Tamura and LRVE models based on volume fraction distribution. For plate analysis, the refined plate theory for functionally graded plates on elastic foundation is proposed to predict buckling and free vibration of thick FG plates. This theory delineates the transverse displacement into both bending and shear parts with only four-unknowns, and therefore decreases the number of governing equations. A sinusoidal variation is elected for all displacements across the thickness which satisfies the stress-free boundary conditions on the upper and lower surfaces of the plate without requiring any shear correction factor. The equations of motion and boundary conditions are derived from Hamilton's principle. Analytical solutions for buckling and free vibration are obtained. Numerical examples are presented and compared with those obtained by classical and third-order plate theories using different homogenization models showing significant deviation in results. The effect of elastic foundation parameters are taken into account for various plate configurations. Finally, the present study shows that structural responses of functionally graded plates can be correctly evaluated by the correct choice of the constituent materials and their homogenization models, which is generally neglected in the vast majority of investigations.

2. Homogenized models for functionally graded materials

As mentioned above, functionally graded materials are non-conventional composite materials. The material properties of FGM plates are assumed to vary continuously through the plate thickness and are dependent on the volume fraction of inclusions. The distribution of material properties is assumed to obey the power-law distribution as follows (Hebali *et al.* 2014, Kar *et al.* 2016)

$$V_f(z) = V_m + (V_c - V_m)\left(\frac{2z+h}{2h}\right)^p \tag{1}$$

where p is the power law index and the subscripts m and c represent the metallic and ceramic constituents, respectively. The homogenization models are deployable for the computation of the Young's modulus $E(z)$ and Poisson's ratio $\upsilon(z)$. In this study, the material non-homogeneous properties are derived via explicit homogenization models such as Voigt, Reuss, Hashin-Shtrikman bounds, Tamura and Cubic local representative volume elements (LRVE) models where the volume fraction is adopted as a law of material distribution through the thickness.

2.1 Voigt rule

This model was derived by Voigt (1889) and is a widely used model for the effective properties of functionally graded materials. It considers a constant strain through the material coordinate loading to predict the homogenization proprieties of heterogonous materials at the macroscopic-scale. Appling the assumption of Voigt for functionally graded materials, the Young's modulus is given as

$$E(z) = E_c V_f(z) + E_m(1 - V_f(z)) \tag{2}$$

and the related Poisson's ratio is assumed as

$$\upsilon(z) = \upsilon_c V_f(z) + \upsilon_m(1 - V_f(z)) \tag{3}$$

2.2 Reuss rule

According to the Reuss assumption (Reuss 1929), the effective proprieties are obtained as a function of constant stress tensor through the material. This model produces estimates of the Young's modulus and Poisson's ratio as

$$E(z) = \frac{E_c E_m}{E_c(1 - V_f(z)) + E_m V_f(z)} \tag{4}$$

and

$$\upsilon(z) = \frac{\upsilon_c \upsilon_m}{\upsilon_c(1 - V_f(z)) + \upsilon_m V_f(z)} \tag{5}$$

Hill (1963) much later showed that the Voigt and Reuss rules present the upper and lower bounds respectively of the elastic effective proprieties of reinforced solids and their assumptions can be derived from the energy principles, as defined by Hill's condition (Hazanov 1998).

2.3 Hashin-Shtrikman bounds model

Hashin and Shtrikman (1963) proposed a variational principle based on strain and stress fields to express the effective elastic proprieties for two-phase materials. This

permitted the geometry and physical propriety of inclusions and therefore provided the lower and upper bounds as a function of the bulk (K) and shear modulus (G). The Young's modulus can been stated in the form

$$E(z)=\frac{9G(z)K(z)}{G(z)+3K(z)} \tag{6}$$

Poisson's ratio is given as

$$\upsilon(z)=\frac{3K(z)-2G(z)}{2G(z)+6K(z)} \tag{7}$$

where *G(z)* and *K(z)* denote the shear and bulk moduli through the thickness respectively

$$\left.\begin{aligned} G^{Low}(z)&=G_m+\frac{V_f(z)}{\frac{1}{G_c-G_m}+\frac{6(K_m+2G_m)(1-V_f(z))}{5G_m(3K_m+4G_m)}}\\ K^{Low}(z)&=K_m+\frac{V_f(z)}{\frac{1}{K_c-K_m}+\frac{3(1-V_f(z))}{(3K_m+4G_m)}} \end{aligned}\right\} \tag{8}$$

for lower bound

and

$$\left.\begin{aligned} G^{Up}(z)&=G_c+\frac{V_f(z)}{\frac{1}{G_m-G_c}+\frac{6(K_c+2G_c)(1-V_f(z))}{5G_c(3K_c+4G_c)}}\\ K^{Up}(z)&=K_c+\frac{V_f(z)}{\frac{1}{K_m-K_c}+\frac{3(1-V_f(z))}{(3K_c+4G_c)}} \end{aligned}\right\} \tag{9}$$

for upper bound

In fact, the upper and lower bounds describe the contrast in material properties or phases of the matrix and inclusions.

2.4 Tamura model

Tamura's model is based on a modified linear mixture rule for two phase materials achieved by introducing the empirical fitting parameter q_T called the "stress-to-strain transfer" (Zuiker 1995, Gasik 1998). This parameter is derived from coupling the stress and strain averages under uniaxial loading of two phase materials. The emerging effective Young's modulus for this model described below

$$E(z)=\frac{(1-V_f(z))E_m(q_T-E_c)+V_f(z)E_c(q_T-E_m)}{(1-V_f(z))(q_T-E_c)+V_f(z)(q_T-E_m)} \tag{10}$$

Moreover, for $q_T=0$ Reuss's model is retrieved as a special case. Furthermore Voigt's model corresponds to the case given by $q_T= \pm\infty$. Poisson's ratio is derived from Voigt's model as

$$\upsilon(z)=\upsilon_c V_f(z)+\upsilon_m(1-V_f(z)) \tag{11}$$

2.5 Cubic local representative volume elements (LRVE) model

By taking into account the interfaces between the constituents of the two phase materials and their geometrical arrangements, Gasik and Lilius (1994) formulated a new micro-mechanical model to predict the effective elastic proprieties based on small cellular mechanical properties. This intermediate scale is termed the cubic local representative volume element (LRVE) which relates the strain and stress components on the local representative element surfaces at the infinite length scale. These assumptions are applied to Young's modulus as follows

$$E(z)=E_m\left(1-\sqrt[3]{V_f(z)}\left(1-\frac{1}{1-\sqrt[3]{V_f(z)}(1-E_m/E_c)}\right)\right) \tag{12}$$

By simplification, the Young's modulus is easily obtained as

$$E(z)=E_m\left(1+\frac{V_f(z)}{FE-\sqrt[3]{V_f(z)}}\right) \tag{13}$$

wherein

$$FE=\frac{1}{1-E_m/E_c} \tag{14}$$

Additionally Poisson's ratio emerges in the same form as for the Voigt model

$$\upsilon(z)=\upsilon_c V_f(z)+\upsilon_m(1-V_f(z)) \tag{15}$$

3. Theoretical formulation

3.1 Kinematics

The displacement field of the present theory is chosen based on the following assumptions: (1) The transverse displacements are partitioned into bending and shear components; (2) the in-plane displacement is partitioned into extension, bending and shear components; (3) the bending parts of the in-plane displacements are similar to those given by CPT ; and (4) the shear parts of the in-plane displacements give rise to the sinusoidal variations of shear strains and hence to shear stresses through the thickness of the plate in such a way that the shear stresses vanish on the top and bottom surfaces of the plate. Based on these assumptions, the following displacement field relations can be obtained

$$u(x,y,z,t)=u_0(x,y,t)-z\frac{\partial w_b}{\partial x}-f(z)\frac{\partial w_s}{\partial x} \tag{16a}$$

$$v(x,y,z,t)=v_0(x,y,t)-z\frac{\partial w_b}{\partial y}-f(z)\frac{\partial w_s}{\partial y} \tag{16b}$$

$$w(x,y,z,t) = w_b(x,y,t) + w_s(x,y,t) \tag{16c}$$

where u_0 and v_0 denote the displacements along the x and y coordinate directions of a point on the mid-plane of the plate; w_b and w_s are the bending and shear components of the transverse displacement, respectively. In this study, the shape function $f(z)$ is chosen based on the sinusoidal function proposed by Touratier (1991) as

$$f(z) = z - \frac{h}{\pi}\sin\left(\frac{\pi z}{h}\right) \tag{17}$$

The non-zero strains associated with the displacement field in Eq. (16) are

$$\begin{Bmatrix}\varepsilon_x\\ \varepsilon_y\\ \gamma_{xy}\end{Bmatrix} = \begin{Bmatrix}\varepsilon_x^0\\ \varepsilon_y^0\\ \gamma_{xy}^0\end{Bmatrix} + z\begin{Bmatrix}k_x^b\\ k_y^b\\ k_{xy}^b\end{Bmatrix} + f(z)\begin{Bmatrix}k_x^s\\ k_y^s\\ k_{xy}^s\end{Bmatrix} \tag{18a}$$

$$\begin{Bmatrix}\gamma_{yz}\\ \gamma_{xz}\end{Bmatrix} = g(z)\begin{Bmatrix}\gamma_{yz}^0\\ \gamma_{xz}^0\end{Bmatrix} \tag{18b}$$

where

$$\begin{Bmatrix}\varepsilon_x^0\\ \varepsilon_y^0\\ \gamma_{xy}^0\end{Bmatrix} = \begin{Bmatrix}\dfrac{\partial u_0}{\partial x}\\ \dfrac{\partial v_0}{\partial x}\\ \dfrac{\partial u_0}{\partial y} + \dfrac{\partial v_0}{\partial x}\end{Bmatrix},\quad \begin{Bmatrix}k_x^b\\ k_y^b\\ k_{xy}^b\end{Bmatrix} = \begin{Bmatrix}-\dfrac{\partial^2 w_b}{\partial x^2}\\ -\dfrac{\partial^2 w_b}{\partial y^2}\\ -2\dfrac{\partial^2 w_b}{\partial x\partial y}\end{Bmatrix},\quad \begin{Bmatrix}k_x^s\\ k_y^s\\ k_{xy}^s\end{Bmatrix} = \begin{Bmatrix}-\dfrac{\partial^2 w_s}{\partial x^2}\\ -\dfrac{\partial^2 w_s}{\partial y^2}\\ -2\dfrac{\partial^2 w_s}{\partial x\partial y}\end{Bmatrix}, \tag{19a}$$

$$\begin{Bmatrix}\gamma_{yz}^0\\ \gamma_{xz}^0\end{Bmatrix} = \begin{Bmatrix}\gamma_{yz}^s\\ \gamma_{xz}^s\end{Bmatrix} \tag{19b}$$

$$g(z) = 1 - \frac{df(z)}{dz} \tag{19c}$$

3.2 Equilibrium equations

Hamilton's principle is used herein to derive equations of motion for plates resting on elastic foundation. The principle can be stated in an analytical form as follows (Zemri *et al.* 2015, Bellifa *et al.* 2017b, Kaci *et al.* 2018, Mokhtar *et al.* 2018)

$$\int_0^T (\delta U + \delta V - \delta K)dt = 0 \tag{20}$$

where δU is the variation of strain energy, δV is the variation of potential energy and δK is the variation of kinetic energy.

The variation of strain energy of the plate is calculated by

$$\begin{aligned}\delta U &= \int_{-h/2}^{h/2}\int_A \left[\sigma_x\delta\varepsilon_x + \sigma_y\delta\varepsilon_y + \tau_{xy}\delta\gamma_{xy} + \tau_{yz}\delta\gamma_{yz} + \tau_{xz}\delta\gamma_{xz}\right]dA\,dz\\ &= \int_A \left[N_x\delta\varepsilon_x^0 + N_y\delta\varepsilon_y^0 + N_{xy}\delta\gamma_{xy}^0 + M_x^b\delta k_x^b + M_y^b\delta k_y^b + M_{xy}^b\delta k_{xy}^b\right.\\ &\quad \left. + M_x^s\delta k_x^s + M_y^s\delta k_y^s + M_{xy}^s\delta k_{xy}^s + S_{yz}^s\delta\gamma_{yz}^0 + S_{xz}^s\delta\gamma_{xz}^0\right]dA = 0\end{aligned} \tag{21}$$

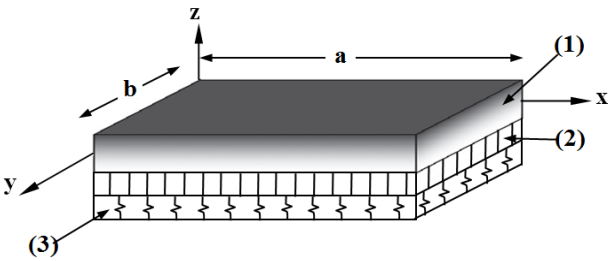

Fig. 1 FGM plate (1) resting on an elastic foundation consisting of shearing (2) and Winkler (3) layers

where A is the top surface and the stress resultants N, M and S are defined by

$$\begin{Bmatrix}N_x, N_y, N_{xy}\\ M_x^b, M_y^b, M_{xy}^b\\ M_x^s, M_y^s, M_{xy}^s\end{Bmatrix} = \int_{-h/2}^{h/2}(\sigma_x,\sigma_y,\tau_{xy})\begin{Bmatrix}1\\ z\\ f(z)\end{Bmatrix}dz, \tag{22}$$

$$(S_{xz}^s, S_{yz}^s) = \int_{-h/2}^{h/2}(\tau_{xz},\tau_{yz})g(z)dz. \tag{23}$$

The variation of potential energy of the applied loads can be expressed thus

$$\delta V = -\int_A \left(N^0 - f_e\right)\delta\left(w_b + w_s\right)dA \tag{24}$$

where f_e is the density of reaction force of the elastic foundation.

$$f_e = K_W\left(w_b + w_b\right)^2 - K_{S1}\frac{\partial^2\left(w_b + w_b\right)}{\partial x^2} - K_{S2}\frac{\partial^2\left(w_b + w_b\right)}{\partial y^2} \tag{25}$$

where K_W and K_S are the *transverse* and *shear stiffness* coefficients of the foundation, respectively and N^0 is the *in-plane* applied load.

$$N^0 = N_x^0\frac{\partial^2\left(w_b + w_b\right)}{\partial x^2} + N_y^0\frac{\partial^2\left(w_b + w_b\right)}{\partial y^2} + 2N_{xy}^0\frac{\partial^2\left(w_b + w_b\right)}{\partial x\partial y} \tag{26}$$

where $N_x{}^0$, $N_y{}^0$ and $N_{xy}{}^0$ are in-plane pre-buckling forces

The variation of kinetic energy of the plate can be written in the form

$$\begin{aligned}\delta K &= \int_{-h/2}^{h/2}\int_A \left[\ddot{u}\delta u + \ddot{v}\delta v + \ddot{w}\delta w\right]\rho(z)\,dA\,dz\\ &= \int_A \left\{I_0\left[\ddot{u}_0\delta u_0 + \ddot{v}_0\delta v_0 + \left(\ddot{w}_b + \ddot{w}_s\right)\left(\delta w_b + \delta w_s\right)\right]\right.\\ &\quad - I_1\left(\ddot{u}_0\frac{\partial\delta w_b}{\partial x} + \frac{\partial\ddot{w}_b}{\partial x}\delta u_0 + \ddot{v}_0\frac{\partial\delta w_b}{\partial y} + \frac{\partial\ddot{w}_b}{\partial y}\delta v_0\right)\\ &\quad - J_1\left(\ddot{u}_0\frac{\partial\delta w_s}{\partial x} + \frac{\partial\ddot{w}_s}{\partial x}\delta u_0 + \ddot{v}_0\frac{\partial\delta w_s}{\partial y} + \frac{\partial\ddot{w}_s}{\partial y}\delta v_0\right)\\ &\quad + I_2\left(\frac{\partial\ddot{w}_b}{\partial x}\frac{\partial\delta w_b}{\partial x} + \frac{\partial\ddot{w}_b}{\partial y}\frac{\partial\delta w_b}{\partial y}\right) + K_2\left(\frac{\partial\ddot{w}_s}{\partial x}\frac{\partial\delta w_s}{\partial x} + \frac{\partial\ddot{w}_s}{\partial y}\frac{\partial\delta w_s}{\partial y}\right)\\ &\quad \left. + J_2\left(\frac{\partial\ddot{w}_b}{\partial x}\frac{\partial\delta w_s}{\partial x} + \frac{\partial\ddot{w}_s}{\partial x}\frac{\partial\delta w_b}{\partial x} + \frac{\partial\ddot{w}_b}{\partial y}\frac{\partial\delta w_s}{\partial y} + \frac{\partial\ddot{w}_s}{\partial y}\frac{\partial\delta w_b}{\partial y}\right)\right\}dA\end{aligned} \tag{27}$$

Here the dot-superscript convention corresponds to differentiation with respect to the time variable, t and (I_0, I_1,

J_1, I_2, J_2, K_2) are mass inertias, defined as follows

$$\left(I_0, I_1, J_1, I_2, J_2, K_2\right) = \int_{-h/2}^{h/2} \left(1, z, f, z^2, z\,f, f^2\right) \rho(z) dz \quad (28)$$

Substituting the expressions for δU, δV, and δK from Eqs. (21), (24), and (27) into Eq. (20) and integrating by parts, and collecting the coefficients of δu_0, δv_0, δw_b and δw_s, the following equations of motion of the plate are obtained

$$\delta u_0 : \ \frac{\partial N_x}{\partial x} + \frac{\partial N_{xy}}{\partial y} = I_0 \ddot{u}_0 - I_1 \frac{\partial \ddot{w}_b}{\partial x} - J_1 \frac{\partial \ddot{w}_s}{\partial x} \quad (29a)$$

$$\delta v_0 : \ \frac{\partial N_{xy}}{\partial x} + \frac{\partial N_y}{\partial y} = I_0 \ddot{v}_0 - I_1 \frac{\partial \ddot{w}_b}{\partial y} - J_1 \frac{\partial \ddot{w}_s}{\partial y} \quad (29b)$$

$$\delta w_b : \ \frac{\partial^2 M_x^b}{\partial x^2} + 2\frac{\partial^2 M_{xy}^b}{\partial x \partial y} + \frac{\partial^2 M_y^b}{\partial y^2} - N^0 - f_e = I_0\left(\ddot{w}_b + \ddot{w}_s\right) + I_1\left(\frac{\partial \ddot{u}_0}{\partial x} + \frac{\partial \ddot{v}_0}{\partial y}\right) - I_2 \nabla^2 \ddot{w}_b - J_2 \nabla^2 \ddot{w}_s \quad (29c)$$

$$\delta w_s : \ \frac{\partial^2 M_x^s}{\partial x^2} + 2\frac{\partial^2 M_{xy}^s}{\partial x \partial y} + \frac{\partial^2 M_y^s}{\partial y^2} + \frac{\partial S_{xz}^s}{\partial x} + \frac{\partial S_{yz}^s}{\partial y} - N^0 - f_e = I_0\left(\ddot{w}_b + \ddot{w}_s\right) + J_1\left(\frac{\partial \ddot{u}_0}{\partial x} + \frac{\partial \ddot{v}_0}{\partial y}\right) - J_2 \nabla^2 \ddot{w}_b - K_2 \nabla^2 \ddot{w}_s \quad (29d)$$

3.3 Constitutive equations

The linear constitutive relations of a FG plate can be written as

$$\begin{Bmatrix} \sigma_x \\ \sigma_y \\ \tau_{yz} \\ \tau_{xz} \\ \tau_{xy} \end{Bmatrix} = \begin{bmatrix} C_{11} & C_{12} & 0 & 0 & 0 \\ C_{12} & C_{22} & 0 & 0 & 0 \\ 0 & 0 & C_{44} & 0 & 0 \\ 0 & 0 & 0 & C_{55} & 0 \\ 0 & 0 & 0 & 0 & C_{66} \end{bmatrix} \begin{Bmatrix} \varepsilon_x \\ \varepsilon_y \\ \gamma_{yz} \\ \gamma_{xz} \\ \gamma_{xy} \end{Bmatrix} \quad (30)$$

where (σ_x, σ_y, τ_{yz}, τ_{xz}, τ_{xy}) and (ε_x, ε_y, γ_{yz}, γ_{xz}, γ_{xy}) are the stress and strain components, respectively. The computation of the elastic constants C_{ij} are the plane stress reduced elastic constants, defined as

$$C_{11} = C_{22} = \frac{E(z)}{1-\nu(z)^2}, \ C_{12} = \nu(z)\, C_{11} \quad (31a)$$

$$C_{44} = C_{55} = C_{66} = G(z) = \frac{E(z)}{2\left(1+\nu(z)\right)}, \quad (31b)$$

E, G and the elastic coefficients C_{ij} vary through the thickness according to Eqs. (2), (4),(6), (10) or (13). By substituting Eq. (18) into Eqs. (30) and the subsequent results into Eqs. (22) and (23), the stress resultants are readily obtained as

$$\begin{Bmatrix} N \\ M^b \\ M^s \end{Bmatrix} = \begin{bmatrix} A & B & B^s \\ B & D & D^s \\ B^s & D^s & H^s \end{bmatrix} \begin{Bmatrix} \varepsilon \\ k^b \\ k^s \end{Bmatrix} \quad (32a)$$

$$S = A^s \gamma \quad (32b)$$

where

$$N = \left\{N_x, N_y, N_{xy}\right\}, \quad M^b = \left\{M_x^b, M_y^b, M_{xy}^b\right\}, \quad M^s = \left\{M_x^s, M_y^s, M_{xy}^s\right\}, \quad (33a)$$

$$\varepsilon = \left\{\varepsilon_x^0, \varepsilon_y^0, \gamma_{xy}^0\right\}, \quad k^b = \left\{k_x^b, k_y^b, k_{xy}^b\right\}, \quad k^s = \left\{k_x^s, k_y^s, k_{xy}^s\right\}, \quad (33b)$$

$$A = \begin{bmatrix} A_{11} & A_{12} & 0 \\ A_{12} & A_{22} & 0 \\ 0 & 0 & A_{66} \end{bmatrix}, \quad B = \begin{bmatrix} B_{11} & B_{12} & 0 \\ B_{12} & B_{22} & 0 \\ 0 & 0 & B_{66} \end{bmatrix}, \quad D = \begin{bmatrix} D_{11} & D_{12} & 0 \\ D_{12} & D_{22} & 0 \\ 0 & 0 & D_{66} \end{bmatrix}, \quad (33c)$$

$$B^s = \begin{bmatrix} B_{11}^s & B_{12}^s & 0 \\ B_{12}^s & B_{22}^s & 0 \\ 0 & 0 & B_{66}^s \end{bmatrix}, \quad D^s = \begin{bmatrix} D_{11}^s & D_{12}^s & 0 \\ D_{12}^s & D_{22}^s & 0 \\ 0 & 0 & D_{66}^s \end{bmatrix}, \quad H^s = \begin{bmatrix} H_{11}^s & H_{12}^s & 0 \\ H_{12}^s & H_{22}^s & 0 \\ 0 & 0 & H_{66}^s \end{bmatrix}, \quad (33d)$$

$$S = \left\{S_{xz}^s, S_{yz}^s\right\}, \quad \gamma = \left\{\gamma_{xz}, \gamma_{yz}\right\}, \quad A^s = \begin{bmatrix} A_{44}^s & 0 \\ 0 & A_{55}^s \end{bmatrix}, \quad (33e)$$

Here the stiffness coefficients are defined as

$$\begin{Bmatrix} A_{11} & B_{11} & D_{11} & B_{11}^s & D_{11}^s & H_{11}^s \\ A_{12} & B_{12} & D_{12} & B_{12}^s & D_{12}^s & H_{12}^s \\ A_{66} & B_{66} & D_{66} & B_{66}^s & D_{66}^s & H_{66}^s \end{Bmatrix} = \int_{-h/2}^{h/2} C_{11} \left(1, z, z^2, f(z), z\,f(z), f^2(z)\right) \begin{Bmatrix} 1 \\ \nu(z) \\ \frac{1-\nu(z)}{2} \end{Bmatrix} dz, \quad (34a)$$

and

$$\left(A_{22}, B_{22}, D_{22}, B_{22}^s, D_{22}^s, H_{22}^s\right) = \left(A_{11}, B_{11}, D_{11}, B_{11}^s, D_{11}^s, H_{11}^s\right) \quad (34b)$$

$$A_{44}^s = A_{55}^s = \int_{-h/2}^{h/2} C_{44} \left[g(z)\right]^2 dz, \quad (34c)$$

3.4 Equations of motion in terms of displacements

Introducing Eq. (34) into Eq. (29), the equations of motion can be expressed in terms of displacements (δu_0, δv_0, δw_b, δw_s) and the appropriate equations take the form

$$A_{11} d_{11} u_0 + A_{66} d_{22} u_0 + \left(A_{12} + A_{66}\right) d_{12} v_0 - B_{11} d_{111} w_b - \left(B_{12} + 2B_{66}\right) d_{122} w_b - \left(B_{12}^s + 2B_{66}^s\right) d_{122} w_s - B_{11}^s d_{111} w_s = I_0 \ddot{u}_0 - I_1 d_1 \ddot{w}_b - J_1 d_1 \ddot{w}_s, \quad (35a)$$

$$A_{22} d_{22} v_0 + A_{66} d_{11} v_0 + \left(A_{12} + A_{66}\right) d_{12} u_0 - B_{22} d_{222} w_b - \left(B_{12} + 2B_{66}\right) d_{112} w_b - \left(B_{12}^s + 2B_{66}^s\right) d_{112} w_s - B_{22}^s d_{222} w_s = I_0 \ddot{v}_0 - I_1 d_2 \ddot{w}_b - J_1 d_2 \ddot{w}_s, \quad (35b)$$

$$\begin{aligned}&B_{11}d_{111}u_0+\left(B_{12}+2B_{66}\right)d_{122}u_0+\left(B_{12}+2B_{66}\right)d_{112}v_0+B_{22}d_{222}v_0\\&-D_{11}d_{1111}w_b-2\left(D_{12}+2D_{66}\right)d_{1122}w_b-D_{22}d_{2222}w_b-D^s_{11}d_{1111}w_s\\&-2\left(D^s_{12}+2D^s_{66}\right)d_{1122}w_s-D^s_{22}d_{2222}w_s-N^0-f_e=I_0\left(\ddot{w}_b+\ddot{w}_s\right)\\&+I_1\left(d_1\ddot{u}_0+d_2\ddot{v}_0\right)-I_2\left(d_{11}\ddot{w}_b+d_{22}\ddot{w}_b\right)-J_2\left(d_{11}\ddot{w}_s+d_{22}\ddot{w}_s\right)\end{aligned} \tag{35c}$$

$$\begin{aligned}&B^s_{11}d_{111}u_0+\left(B^s_{12}+2B^s_{66}\right)d_{122}u_0+\left(B^s_{12}+2B^s_{66}\right)d_{112}v_0+B^s_{22}d_{222}v_0-D^s_{11}d_{1111}w_b\\&-2\left(D^s_{12}+2D^s_{66}\right)d_{1122}w_b-D^s_{22}d_{2222}w_b-H^s_{11}d_{1111}w_s\\&-2\left(H^s_{12}+2H^s_{66}\right)d_{1122}w_s-H^s_{22}d_{2222}w_s+A^s_{44}d_{11}w_s+A^s_{55}d_{22}w_s-N^0-f_e=I_0\left(\ddot{w}_b+\ddot{w}_s\right)\\&+J_1\left(d_1\ddot{u}_0+d_2\ddot{v}_0\right)-J_2\left(d_{11}\ddot{w}_b+d_{22}\ddot{w}_b\right)-K_2\left(d_{11}\ddot{w}_s+d_{22}\ddot{w}_s\right)\end{aligned} \tag{35d}$$

where d_{ij}, d_{ijl} and d_{ijlm} are the following differential operators

$$d_{ij}=\frac{\partial^2}{\partial x_i\partial x_j},\quad d_{ijl}=\frac{\partial^3}{\partial x_i\partial x_j\partial x_l},\quad d_{ijlm}=\frac{\partial^4}{\partial x_i\partial x_j\partial x_l\partial x_m},\quad (i,j,l,m=1,2). \tag{35e}$$

3.5 Analytical solutions

Consider a simply supported rectangular plate with length a and width b resting on elastic foundations (Fig. 1). Based on the Navier solution method, the following expansions of displacements (u_0, v_0, w_b, w_s) are assumed as

$$\begin{Bmatrix}u_0\\v_0\\w_b\\w_s\end{Bmatrix}=\sum_{m=1}^{\infty}\sum_{n=1}^{\infty}\begin{Bmatrix}U_{mn}e^{i\omega t}\cos(\lambda x)\sin(\mu y)\\V_{mn}e^{i\omega t}\sin(\lambda x)\cos(\mu y)\\W_{bmn}e^{i\omega t}\sin(\lambda x)\sin(\mu y)\\W_{smn}e^{i\omega t}\sin(\lambda x)\sin(\mu y)\end{Bmatrix} \tag{36}$$

where U_{mn}, V_{mn}, W_{bmn}, W_{smn} unknown parameters must be determined, ω is the eigen-frequency associated with $(m,n)^{\text{th}}$eigen-mode, and $\lambda=m\pi/a$ and $\mu=n\pi/b$. Substituting Eq. (36) into Eq. (35), the analytical solutions can be obtained from the matrix-vector system

$$\left(\begin{bmatrix}a_{11}&a_{12}&a_{13}&a_{14}\\a_{12}&a_{22}&a_{23}&a_{24}\\a_{13}&a_{23}&a_{33}+k&a_{34}+k\\a_{14}&a_{24}&a_{34}+k&a_{44}+k\end{bmatrix}-\omega^2\begin{bmatrix}m_{11}&0&m_{13}&m_{14}\\0&m_{22}&m_{23}&m_{24}\\m_{13}&m_{23}&m_{33}&m_{34}\\m_{14}&m_{24}&m_{34}&m_{44}\end{bmatrix}\right)\begin{Bmatrix}U_{mn}\\V_{mn}\\W_{bmn}\\W_{smn}\end{Bmatrix}=\begin{Bmatrix}0\\0\\0\\0\end{Bmatrix} \tag{37}$$

in which

$$\begin{aligned}&a_{11}=-\left(A_{11}\lambda^2+A_{66}\mu^2\right)\quad a_{12}=-\lambda\mu\left(A_{12}+A_{66}\right)\quad a_{13}=\lambda\left[B_{11}\lambda^2+\left(B_{12}+2B_{66}\right)\mu^2\right]\\&a_{14}=\lambda\left[B^s_{11}\lambda^2+\left(B^s_{12}+2B^s_{66}\right)\mu^2\right]\quad a_{22}=-\left(A_{66}\lambda^2+A_{22}\mu^2\right)\\&a_{23}=\mu\left[\left(B_{12}+2B_{66}\right)\lambda^2+B_{22}\mu^2\right]\quad a_{24}=\mu\left[\left(B^s_{12}+2B^s_{66}\right)\lambda^2+B^s_{22}\mu^2\right]\\&a_{33}=-\left(D_{11}\lambda^4+2\left(D_{12}+2D_{66}\right)\lambda^2\mu^2+D_{22}\mu^4+K_W+K_S\left(\lambda^2+\mu^2\right)\right)\\&a_{34}=-\left(D^s_{11}\lambda^4+2\left(D^s_{12}+2D^s_{66}\right)\lambda^2\mu^2+D^s_{22}\mu^4+K_W+K_S\left(\lambda^2+\mu^2\right)\right)\\&a_{44}=-\left(H^s_{11}\lambda^4+2\left(H^s_{11}+2H^s_{66}\right)\lambda^2\mu^2+H^s_{22}\mu^4+A^s_{55}\lambda^2+A^s_{44}\mu^2+K_W+K_S\left(\lambda^2+\mu^2\right)\right)\end{aligned} \tag{38}$$

$$m_{11}=m_{22}=-I_0,\ m_{13}=\lambda I_1,\ m_{14}=\lambda J_1,\ m_{23}=\mu I_1,\ m_{24}=\mu J_1,\ m_{33}=-\left(I_0+I_2\left(\lambda^2+\mu^2\right)\right),$$
$$m_{34}=-\left(I_0+J_2\left(\lambda^2+\mu^2\right)\right),\ m_{44}=-\left(I_0+K_2\left(\lambda^2+\mu^2\right)\right),$$

$$k=N_{cr}\left(\gamma_1\lambda^2+\gamma_2\mu^2\right)$$

4. Results and discussion

In this section, various numerical examples are presented and compared to verify the effect of the homogenization models in predicting the critical buckling loads and natural frequencies of simply supported functionally graded plates resting on elastic foundation. The material properties of FGM plates used in this study are listed in Table 1. The effective mass density $\rho(z)$ is estimated using the power-law distribution with Voigt's rule of mixtures for all the models as follows

$$\rho(z)=\rho_m+\left(\rho_c-\rho_m\right)\left(\frac{2z+h}{2h}\right)^k \tag{39}$$

For convenience, the following dimensionless forms are utilized

$$\begin{aligned}&\overline{N}=N_{cr}\frac{a^2}{E_mh^3},\ \widehat{N}=N_{cr}\frac{a^2}{100h^3},\ \overline{\omega}=\omega\frac{a^2}{h}\sqrt{\rho_m/E_m},\\&K_0=\frac{a^4K_W}{D_m},\ K_1=\frac{a^2K_S}{D_m},\ D_m=\frac{h^3E_m}{12\left(1-\upsilon_m^2\right)}\end{aligned} \tag{40}$$

Table 1 Material properties used in the FGM plate

Properties	Metal aluminum Alloy 1100	Ceramic Alumina (Al_2O_3)
E (GPa)	69	380
v	0.33	0.22
ρ (kg/m^3)	2710	3980

Table 2 Comparison of non-dimensional critical unidirectional buckling loads $\overline{N}$ of simply supported FGM square plate with different homogenization models ($a/h=5$)

p	Theory	Homogenization model					
		Voigt	Reuss	Hashin (LB)	Hashin (UB)	LRVE	Tamura
Ceramic	CPT [a]	19.0406	19.0406	19.0406	19.0406	19.0406	19.0406
	TSDT [a]	15.8412	15.8412	15.8412	15.8412	15.8412	15.8412
	Present SSDT	15.8458	15.8458	15.8458	15.8458	15.8458	15.8458
0.5	CPT [a]	12.5797	8.4890	9.7010	11.1882	9.8634	9.9060
	TSDT [a]	10.6123	7.0776	8.1266	9.4558	8.31763	8.3275
	Present SSDT	10.6187	7.0775	8.1283	9.4601	8.31971	8.3297
1	CPT [a]	9.7521	7.0908	7.8269	8.7725	7.8687	7.9529
	TSDT [a]	8.2480	5.7897	6.4648	7.3851	6.54682	6.6012
	Present SSDT	8.2496	5.7872	6.4630	7.3855	6.54529	6.6000
2	CPT [a]	7.6581	6.2143	6.6734	7.1760	6.7266	6.7446
	TSDT [a]	6.3768	4.9214	5.3436	5.8941	5.4005	5.4274
	Present SSDT	6.3746	4.9181	5.3391	5.8906	5.3949	5.4229
10	CPT [a]	5.9343	4.8381	5.2004	5.5997	5.2570	5.2582
	TSDT [a]	4.4905	3.7655	3.9997	4.2662	4.0335	4.0384
	Present SSDT	4.4862	3.7652	4.0000	4.2649	4.0345	4.0388
Metal	CPT [a]	3.6921	3.6921	3.6921	3.6921	3.6921	3.6921
	TSDT [a]	2.9895	2.9895	2.9895	2.9895	2.9895	2.9895
	Present SSDT	2.9904	2.9904	2.9904	2.9904	2.9904	2.9904

[a] Given by Akbarzadeh *et al.* (2015)

Table 3 Comparison of non-dimensional critical unidirectional buckling loads $\bar{N}$ of simply supported FGM square plate with different homogenization models (a/h=10)

p		Homogenization model					
		Voigt	Reuss	Hashin (LB)	Hashin (UB)	LRVE	Tamura
ceramic	CPT [a]	19.0406	19.0406	19.0406	19.0406	19.0406	19.0406
	TSDT [a]	18.1238	18.1238	18.1238	18.1238	18.1238	18.1238
	Present SSDT	18.1243	18.1243	18.1243	18.1243	18.1243	18.1243
0.5	CPT [a]	12.5797	8.4890	9.7010	11.1882	9.8634	9.906
	TSDT [a]	12.0216	8.0851	9.2520	10.6973	9.4246	9.457
	Present SSDT	12.0263	8.0851	9.2530	10.7002	9.4257	9.4584
1	CPT [a]	9.7521	7.0908	7.8269	8.77254	7.8687	7.9529
	TSDT [a]	9.3261	6.7128	7.4344	8.37822	7.4898	7.5648
	Present SSDT	9.3262	6.7113	7.4332	8.37786	7.4887	7.5638
2	CPT [a]	7.6581	6.2143	6.6734	7.17600	6.7266	6.7446
	TSDT [a]	7.2910	5.8304	6.2815	6.80511	6.3366	6.3579
	Present SSDT	7.2897	5.8283	6.2793	6.80332	6.3339	6.3557
10	CPT [a]	5.9343	4.8381	5.2004	5.59969	5.2570	5.2582
	TSDT [a]	5.4916	4.5156	4.8364	5.19273	4.8855	4.8880
	Present SSDT	5.4890	4.5123	4.8346	5.19094	4.8842	4.8864
Metal	CPT [a]	3.6921	3.4868	3.6921	3.6921	3.6921	3.6921
	TSDT [a]	3.4868	3.4868	3.4868	3.4868	3.6921	3.4868
	Present SSDT	3.4870	3.4870	3.4870	3.4870	3.4870	3.4870

[a] Given by Akbarzadeh *et al.* (2015)

4.1 Results for buckling analysis

The first example deals with thick ($a/h = 5$) functionally graded square plates. Various values of the material index $p$are considered. Young's modulus is evaluated using the homogenization models described above. The obtained results are compared with classical and third order plate theory documented in Akbarzadeh *et al.* (2015). Table 2 presents the computed non-dimensional critical buckling loads $\bar{N}$. It is pertinent to note that the classical plate theory solutions neglect the effect of transverse shear strains and this assumption tends to *over-estimate* the non-dimensional critical buckling loads for thick FGM plates. The third order plate theory solutions are obtained based on parabolic variation of *in-plane* displacement through the plate thickness by using five unknown parameters.

Inspection of Table 2 demonstrates that the present computations are in very good agreement with third order plate theory solutions available in the literature for all homogenization models with only four parameters. On the other hand, it is observed that for all homogenization models, the non-dimensional critical buckling loads decrease as a function of material index parameters. The non-dimensional critical buckling loads are highest in the ceramic phase and lowest for the metal phase. Additionally, from a comparison of the homogenisation models a deviation is observed in the computed non-dimensional critical buckling loads for Voigt, Reuss and Hashin Upper bounds models.

However closer correlation is achieved with the Hashin Lower bounds, LRVE and Tamura models which exhibit good similarity, the maximum values of non-dimensional critical buckling load correspond to Voigt's model which estimates the effective proprieties provided by the upper bounds. The minimum values are produced by Reuss's model which provides approximate estimates of the effective proprieties based on lower bounds. Hashin's upper bounds model estimates the effective proprieties based on optimal shear and bulk moduli for upper phase material, which explains the close values of the results obtained by Voigt's model. For Hashin's lower bounds, LRVE and Tamura models, the effective proprieties are derived as functions of the lower phase material, manifesting in closely correlating values for non-dimensional critical buckling loads. As mentioned above, both Tamura and LRVE models use the same Poisson's ratio estimation and this generates very close results.

Next FGM plates with thickness ratio a/h=10 are analysed, another situation of relevance to aircraft and spacecraft structures. In this scenario, Young's modulus and Poisson ratio are evaluated using Voigt, Reuss and Hashin Upper bounds, Hashin Lower bounds, LRVE and Tamura models. This example aims to predict the non-dimensional critical buckling loads for moderately thick plates; the obtained results are compared with CPT and those predicted by third order plate theory in Table 3.

It is observed that the non-dimensional critical buckling loads are slight higher compared to thick FGM plates. The higher values of non-dimensional critical buckling loads are observed in the ceramic rich phase and decreased to lower magnitudes in the metallic rich phase. The obtained results demonstrate that the same accuracy is achievable with the present theory using a lower number of unknowns than third order theory used by Akbarzadeh *et al.*(2015).The comparison between solutions generated with the different homogenization models show important differences in the computed non-dimensional critical buckling load values. Moreover, the effect of homogenization models does not depend on the thickness ratio of plates; there are various factors such as material phase location and arrangement, zones of graded microstructure and interphase of continuous matrix and inclusions distribution that involve predicting the homogenized effective proprieties and incorporation of these may improve the accuracy of predicted critical buckling loads for FGM plates.

4.2 Results for free vibration analysis

The accuracy of the proposed higher order shear plate theory and the effect of homogenization models are also verified and discussed for a structural dynamic case, namely free vibration analysis. This example is performed for thick and moderately thick FGM square plates. This example aims to verify the effect of homogenization models on fundamental frequency; the obtained results are compared with the classical and third order plate theory solutions of

Table 4 Comparison of non-dimensional fundamental frequency $\bar{\omega}$ of simply supported FGM square plate with different homogenization models (*a/h=5*)

p		Homogenization model					
		Voigt	Reuss	Hashin (LB)	Hashin (UB)	LRVE	Tamura
Ceramic	CPT [a]	10.9571	10.9571	10.9571	10.9571	10.9571	10.9571
	TSDT [a]	10.0885	10.0885	10.0885	10.0885	10.0885	10.0885
	Present SSDT	10.0897	10.0898	10.0898	10.0898	10.0898	10.0898
0.5	CPT [a]	9.4189	7.7166	8.2564	8.8759	8.3253	7.7238
	TSDT [a]	8.7277	7.1185	7.6305	8.2334	7.7172	7.7238
	Present SSDT	8.7301	7.1185	7.6313	8.2346	7.7178	7.7248
1	CPT [a]	8.5358	7.2682	7.6362	8.0892	7.6542	7.6978
	TSDT [a]	7.9227	6.6432	7.0157	7.4944	7.0561	7.0879
	Present SSDT	7.9233	6.6415	7.0151	7.4947	7.0554	7.0874
2	CPT [a]	7.7910	7.0298	7.2771	7.5417	7.3025	7.3149
	TSDT [a]	7.1877	6.3369	6.5952	6.9152	6.6273	6.6446
	Present SSDT	7.1868	6.3345	6.5927	6.9135	6.6242	6.6424
10	CPT [a]	7.2220	6.5423	6.7778	7.0248	6.81379	6.8144
	TSDT [a]	6.3804	5.8474	6.0267	6.2222	6.0524	6.0556
	Present SSDT	6.3773	5.8468	6.0271	6.2212	6.0530	6.0556
Metal	CPT [a]	5.8472	5.8472	5.8472	5.8472	5.8472	5.8472
	TSDT [a]	5.3172	5.3172	5.3172	5.3172	5.3172	5.3172
	Present SSDT	5.3183	5.3179	5.3179	5.3179	5.3179	5.3179

[a] Given by Akbarzadeh *et al.* (2015)

Table 5 Comparison of non-dimensional fundamental frequency $\bar{\omega}$ of simply supported FGM square plate with different homogenization models (*a/h=10*)

p		Homogenization model					
		Voigt	Reuss	Hashin (LB)	Hashin (UB)	LRVE	Tamura
Ceramic	CPT [a]	11.2199	11.2199	11.2199	11.2199	11.2199	11.2199
	TSDT [a]	10.9548	10.9548	10.9548	10.9548	10.9548	10.9548
	Present SSDT	10.9548	10.9549	10.9549	10.9549	10.9549	10.9549
0.5	CPT [a]	9.6468	7.9193	8.4676	9.0959	8.5382	8.5569
	TSDT [a]	9.4370	7.7349	8.2757	8.9005	8.3524	8.3671
	Present SSDT	9.4389	7.7347	8.2761	8.9018	8.3526	8.3678
1	CPT [a]	8.7542	7.4621	7.8399	8.3012	7.8601	7.9028
	TSDT [a]	8.5671	7.2673	7.6475	8.1188	7.6751	7.7141
	Present SSDT	8.5675	7.2664	7.6469	8.1187	7.6746	7.7135
2	CPT [a]	8.0089	7.2176	7.4775	7.7527	7.5063	7.517
	TSDT [a]	7.8215	6.9987	7.2623	7.5569	7.2932	7.3059
	Present SSDT	7.8207	6.9979	7.2608	7.5561	7.2915	7.3049
10	CPT [a]	7.4243	6.7091	6.9544	7.2143	6.9920	6.9927
	TSDT [a]	7.1517	6.4889	6.7147	6.9562	6.7486	6.7503
	Present SSDT	7.1501	6.4863	6.7133	6.9550	6.7475	6.7488
Metal	CPT [a]	5.9875	5.9875	5.9875	5.9875	5.9875	5.9875
	TSDT [a]	5.8237	5.8237	5.8237	5.8237	5.8237	5.8237
	Present SSDT	5.8238	5.8238	5.8238	5.8238	5.8238	5.8238

[a] Given by Akbarzadeh *et al.* (2015)

Akbarzadeh *et al.* (2015). Young's modulus and Poisson's ratio are evaluated using Voigt, Reuss and Hashin Upper bounds, Hashin Lower bounds, LRVE and Tamura models. The mass density has been derived from Voigt's model for all models considered.

The non-dimensional fundamental frequency $\bar{\omega}$ is given in Tables 4 and 5 for different values of the material index parameters.

It is evident that the present computations are in an excellent agreement with the third order plate theory solutions. Since the classical plate theory omits shear deformation effects, it therefore noticeably *over-estimates* the frequency of thick plates. It can be seen that the derived solutions are however close since the dynamic properties of the FGM plates are computed via the same homogenization model. Since increasing material index parameter decreases fundamental frequency values, the highest values are presented in ceramic material phase and the lowest values are observed in the metallic phase according to the effective elasticity modulus and the mass densities of each material can be calculated.

4.3 Parametric study

After proving the authenticity of the present analytical solutions, new results are presented to conduct a parametric study. The critical buckling loads and the fundamental frequency of simply supported functionally graded plates with various material index and elastic foundation parameters are investigated in this section, for all the homogenization models mentioned above.

Table 6 shows the effect of material index and elastic foundation parameters on the critical buckling loads of simply supported FGM square plate with thickness ratio *a*/*h*=10 using Voigt, Reuss and Hashin Upper bounds, Hashin Lower bounds, LRVE and Tamura models.

As can be seen, the obtained non-dimensional critical buckling loads increase as the foundation parameters increase and the *Pasternak parameter* exerts a greater effect compared with the Winkler parameter. It is also observed that the difference between maximum values obtained by Voigt's model and the minimum values obtained by Reuss's model is more significant and decreases when material index parameter increases.

The first four non-dimensional natural frequencies of simply supported square FGM plates for different values of material index parameters and foundation parameters are listed in Tables 7-8 with thickness ratio *a/h*=10. It should be noted that the both mass distribution and mass moment of

Table 6 Effect of the volume fraction exponent and elastic foundation parameters on non-dimensional critical unidirectional buckling loads $\overline{N}$ of simply supported FGM square plate with different homogenization models (a/h=10)

K_0	K_1	Model	Index parameter p					
			Ceramic	0.5	1	2	10	metal
100	0	Voigt	19.0719	12.9738	10.2737	8.2372	6.4365	4.4345
		Reuss	19.0719	9.0326	7.6588	6.7758	5.4597	4.4345
		Hashin (UB)	19.0719	11.6477	9.3254	7.7509	6.1384	4.4345
		Hashin (LB)	19.0719	10.2006	8.3807	7.2268	5.7822	4.4345
		LRVE	19.0719	10.3732	8.4362	7.2814	5.8317	4.4345
		Tamura	19.0719	10.4059	8.5113	7.3032	5.8339	4.4345
0	100	Voigt	36.8278	30.7297	28.0297	25.9932	24.1925	22.1904
		Reuss	36.8278	26.7886	25.4148	24.5317	23.2157	22.1904
		Hashin (UB)	36.8278	29.4036	27.0813	25.5068	23.8945	22.1904
		Hashin (LB)	36.8278	27.9565	26.1367	24.9828	23.5381	22.1904
		LRVE	36.8278	28.1291	26.1922	25.0374	23.5877	22.1904
		Tamura	36.8278	28.1619	26.2672	25.0591	23.5899	22.1904
100	100	Voigt	37.7754	31.6772	28.9772	26.9407	25.1400	23.1380
		Reuss	37.7754	27.7361	26.3623	25.4793	24.1632	23.1380
		Hashin (UB)	37.7754	30.3512	28.0288	26.4543	24.8419	23.1380
		Hashin (LB)	37.7752	28.9041	27.0842	25.9303	24.4857	23.1380
		LRVE	37.7754	29.0767	27.1397	25.9849	24.5352	23.1380
		Tamura	37.7754	29.1094	27.2148	26.0067	24.5374	23.1380

inertia are computed by Voigt's model for all presented homogenization models. It is apparent that the effect of *Pasternak* parameter is higher than that of the *Winkler* parameter. In fact, the difference in obtained fundamental frequency values is minor compared to buckling loads, and decreases with increasing material index parameters. This is due to the material phases transforming from the fully ceramic phase to the fully metal phase which involves a marked depletion in the stiffness and mass density.

In order to verify the effect of homogenization models on the second and third natural frequencies, a simply supported FGM plate with different aspect ratio *(a/b)* is now investigated. From the results presented in Table 9, it

Table 7 Effect of the volume fraction exponent and elastic foundation parameters on the first and second non-dimensional natural frequencies $\overline{\omega}$ of simply supported FGM square plate with different homogenization models (a/h=10)

Mode	K_0	K_1	p	Homogenization model					
				Voigt	Reuss	Hashin (LB)	Hashin (UB)	LRVE	Tamura
1	0	50	0.5	12.5842	11.3588	11.7352	12.1855	11.7891	11.8000
			1	12.1239	11.2415	11.4907	11.8102	11.5084	11.5352
			10	11.7565	11.3697	11.4998	11.6408	11.5197	11.5204
	50	00	0.5	9.62280	7.95823	8.48535	9.09641	8.56003	8.57456
			1	8.78199	7.51858	7.88683	8.34494	7.91360	7.95157
			10	7.45233	6.81849	7.03470	7.26544	7.06735	7.06873
	50	50	0.5	12.7230	11.5121	11.8837	12.3286	11.9370	11.9477
			1	12.2767	11.4060	11.6517	11.9669	11.6692	11.6955
			10	11.9426	11.5623	11.6902	11.8288	11.7098	11.7105
	100	100	0.5	15.3184	14.3256	14.6268	14.9916	14.6700	14.6789
			1	15.1008	14.4008	14.5959	14.8491	14.6093	14.6309
			10	15.3006	15.0096	15.1076	15.2137	15.1227	15.1231

Table 7 Continued

Mode	K_0	K_1	p	Homogenization model					
				Voigt	Reuss	Hashin (LB)	Hashin (UB)	LRVE	Tamura
2	0	50	0.5	49.0973	40.0882	42.9662	46.7916	43.9809	43.7340
			1	45.4100	36.4749	39.0966	42.9025	39.9008	39.8148
			10	31.9747	28.9803	29.7125	30.9809	29.8569	29.9250
	50	0	0.5	49.0973	40.0882	42.9662	46.7916	43.9809	43.7340
			1	45.4100	36.4749	39.0966	42.9025	39.9008	39.8148
			10	31.9747	28.9803	29.7125	30.9809	29.8569	29.9250
	50	50	0.5	49.0973	40.0882	42.9662	46.7916	43.9809	43.7340
			1	45.4100	36.4749	39.0966	42.9025	39.9008	39.8148
			10	31.9747	28.9803	29.7125	30.9809	29.8569	29.9250
	100	100	0.5	49.0973	40.0882	42.9662	46.7916	43.9809	43.7340
			1	45.4100	36.4749	39.0966	42.9025	39.9008	39.8148
			10	31.9747	28.9803	29.7125	30.9809	29.8569	29.9250

Table 8 Effect of the volume fraction exponent and elastic foundation parameters on the third and fourth non-dimensional natural frequencies $\overline{\omega}$ of simply supported FGM square plate with different homogenization models (a/h=10)

Mode	K_0	K_1	p	Homogenization model					
				Voigt	Reuss	Hashin (LB)	Hashin (UB)	LRVE	Tamura
3	0	50	0.5	80.1431	64.9300	70.3691	75.8716	71.5855	71.1993
			1	74.6903	59.5805	64.5357	70.0153	65.4312	65.3296
			10	54.1610	49.3049	50.6597	52.4053	50.7725	50.8936
	50	00	0.5	80.1431	64.9292	70.3682	75.8716	71.5846	71.1989
			1	74.6894	59.5792	64.5344	70.0145	65.4299	65.3292
			10	54.1593	49.3049	50.6588	52.4040	50.7721	50.8932
	50	50	0.5	80.1431	64.9300	70.3691	75.8716	71.5855	71.1993
			1	74.6903	59.5805	64.5357	70.0153	65.4312	65.3296
			10	54.1610	49.3049	50.6597	52.4053	50.7729	50.8940
	100	100	0.5	80.1435	64.9313	70.3704	75.8721	71.5859	71.2006
			1	74.6907	59.5818	64.5370	70.0162	65.4325	65.3309
			10	54.1627	49.3053	50.6601	52.4066	50.7734	50.8945
4	0	50	0.5	366.254	285.723	311.885	346.181	321.454	318.807
			1	332.439	251.162	273.884	308.748	280.450	280.185
			10	204.129	196.167	197.790	200.953	197.632	198.215
	50	0	0.5	366.253	285.720	311.883	346.180	321.452	318.806
			1	332.437	251.160	273.882	308.747	280.448	280.182
			10	204.126	196.164	197.787	200.950	197.629	198.213
	50	50	0.5	366.254	285.723	311.885	346.181	321.454	318.807
			1	332.439	251.163	273.884	308.748	280.450	280.185
			10	204.129	196.167	197.790	200.953	197.632	198.216
	100	100	0.5	366.256	285.724	311.887	346.184	321.456	318.809
			1	332.441	251.164	273.886	308.750	280.453	280.186
			10	204.133	196.170	197.793	200.956	197.635	198.219

can be seen that for all used homogenization models, the

Table 9 Effect of the volume fraction exponent and aspect ratio (a/b) on the second and third non-dimensional natural frequencies $\overline{\omega}$ of simply supported FGM plates with different homogenization models (a/h=10)

Mode	a/b	p	Homogenization model					
			Voigt	Reuss	Hashin (LB)	Hashin (UB)	LRVE	Tamura
2	2	0.5	77.6299	63.3850	67.9354	73.9837	69.5397	69.1496
		1	71.7999	57.6718	61.8175	67.8346	63.0888	62.9526
		10	50.5563	45.8217	46.9793	48.9849	47.2081	47.3157
	3	0.5	109.785	89.6400	96.0757	104.629	98.3442	97.7916
		1	101.540	81.5606	87.4230	95.9326	89.2210	89.0285
		10	71.4977	64.8020	66.4388	69.2755	66.7618	66.9140
	4	0.5	143.142	116.877	125.267	136.420	128.226	127.505
		1	132.392	106.341	113.985	125.081	116.329	116.079
		10	93.2218	84.4911	86.6264	90.3237	87.0467	87.2452

Table 9 Continued

Mode	a/b	p	Homogenization model					
			Voigt	Reuss	Hashin (LB)	Hashin (UB)	LRVE	Tamura
3	2	0.5	126.629	102.341	111.001	119.805	112.928	112.334
		1	117.843	93.8613	101.660	110.383	103.043	102.925
		10	85.2781	77.9209	80.0039	82.6525	80.1743	80.3611
	3	0.5	178.871	143.983	156.365	169.056	159.101	158.294
		1	166.061	131.949	142.885	155.355	144.768	144.697
		10	119.799	110.110	112.923	116.417	113.147	113.399
	4	0.5	232.837	186.394	202.768	219.741	206.350	205.361
		1	215.431	170.641	184.725	201.202	187.048	187.125
		10	154.838	143.411	146.845	150.974	147.105	147.417

second and third non-dimensional natural frequencies increase as aspect ratio increases and when the material index parameter increases, both the second and third non-dimensional natural frequencies decrease.

The effects of the elastic foundation parameters and aspect ratio (b/a) on non-dimensional critical buckling loads

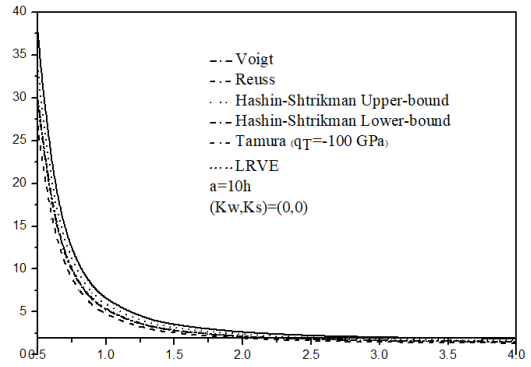

(a) K_w=K_s=0

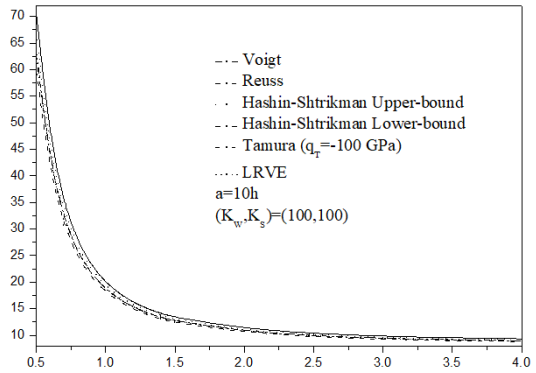

(b) K_w=100, K_s=100

Fig. 2 Variation of non-dimensional critical buckling loads versus the aspect ratio (b/a) of Al/Al_2O_3 square plates (a/h=10, p=1)

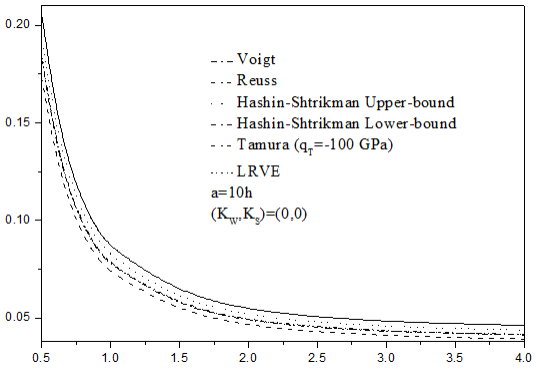

(a) K_w=K_s=0

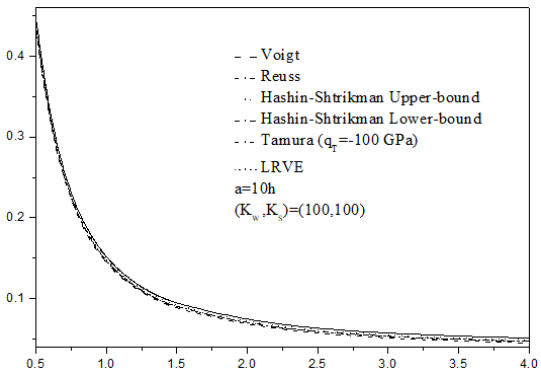

(b) K_w=100, K_s=100

Fig. 3 Variation of non-dimensional fundamental frequency versus the aspect ratio (b/a) of Al/Al_2O_3 square plates (a/h=10, p=1)

are illustrated in Fig. 2 for all presented homogenization models. Evidently the non-dimensional critical buckling loads decrease for FGM plates with higher aspect ratio b/a. Furthermore the effect of Pasternak foundation parameter is more significant than Winkler foundation parameter. It is also observed that the non-dimensional critical buckling loads obtained by Hashin Lower bounds, LRVE and Tamura homogenization models are in much closer agreement than those computed with the other homogenization models employed in this study.

Fig. 3 shows the effect of the elastic foundation parameters and aspect ratio (b/a) on non-dimensional fundamental frequency obtained by using different homogenization models. It is observed that the obtained fundamental frequency decreases when the aspect ratio, b/a, is increased for all models. It should be noted that the all models have used the same mass distribution and mass moment of inertia model and this contributes to a reduction in the difference between computed fundamental frequency generated with the homogenization models studied.

5. Conclusions

A theoretical study of the effect of various homogenization models is presented for buckling and free vibration analyses of functionally graded material (FGM) plates resting on elastic foundations. The accuracy of the present theory has been demonstrated for both buckling and free vibration analyses of simply supported FGM plates. The theory incorporates the shear deformation effect without requiring a shear correction factor. By dividing the transverse displacement into bending and shear components, the number of unknowns and governing equations emerging in the present theory is reduced to four and this refined theory is therefore somewhat simpler than alternate theories available in the scientific literature. The equations of motion derived from Hamilton's principle are solved analytically via Navier's expansion technique for buckling and free vibration problems of a simply supported plate. The present computations have highlighted some important observations:

• The homogenization effect is *non-trivial* and needs to be taken into consideration in order to derive the effective elastic properties that are more physically realistic for engineering applications.

• Since the majority of existing studies use Voigt's model to study FGM plate structural/dynamic behavior, it is logical to explore alternative homogenization models such as Voigt, Reuss and Hashin Upper bounds, Hashin Lower bounds, LRVE and Tamura approaches. These different models invariably yield different results since each model is founded on different assumptions and specific criteria.

• Voigt's model estimates the effective proprieties based on upper bounds considering the ceramic rich phase and generates maximum values for plate responses with markedly lower values obtained by Reuss's model which is based on lower bounds considering a metal rich phase.

• Hashin-Strickman's models derive the effective elastic proprieties from shear and bulk moduli for upper and lower bounds and these produce a moderate agreement with the values computed using the Voigt and Reuss models

respectively.

• Tamura's model derives effective properties from a modification of the Voigt model which includes an empirical fitting parameter q_T based on the nature of matrix-inclusions phases, which is considered as a correction factor to the Voigt model.

• The LRVE model takes into account the small cellular mechanical properties to predict the effective proprieties at the macroscopic-scale for two phase materials and is generally used for random distribution materials or interphase regions.

• In the structural dynamic (free vibration) analysis, the homogenization effect is reasonable since all presented models use the same Voigt's model to predict both the mass distribution and mass moment of inertia.

• In addition, it is observed that increasing material index parameter decreases both critical buckling loads and fundamental frequency and in addition this effect is also observed when aspect ratio (*b/a*) increases. The effect of Pasternak foundation parameter is more prominent than the Winkler foundation parameter on critical buckling loads and fundamental frequency magnitudes.

Finally, the current study provides a good foundation for extension to more general computational simulation for more complex geometrical configurations such as shells structures (Zine *et al.* 2018, Karami *et al.* 2018) and very thick plates (Bousahla *et al.* 2014, Belabed *et al.* 2014, Hebali *et al.* 2014, Bennai *et al.* 2015, Meradjah *et al.* 2015, Larbi Chaht *et al.* 2015, Hamidi *et al.* 2015, Bourada *et al.* 2015, Bennoun *et al.* 2016, Draiche *et al.* 2016, Bouafia *et al.* 2017). In this regard the methodology described furnishes a good pathway for predicting the various effective elastic proprieties and it is hoped that readers may also be encouraged to consider experimental tests to validate the homogenization models considered in to establish the optimum choice for functionally graded plate problems. Also another possible extension of the current work is to consider micro-structural material behaviour which could be simulated within the framework of Eringen's micropolar elastic models for both static and dynamic loading (Othman *et al.* 2013). This could also lead to investigations of fracture propagation in FGM plates with different homogenization models elaborated in this article.

References

Abdelaziz, H.H., Ait Amar Meziane, M., Bousahla, A.A., Tounsi, A., Mahmoud, S.R. and Alwabli, A.S. (2017), "An efficient hyperbolic shear deformation theory for bending, buckling and free vibration of FGM sandwich plates with various boundary conditions", *Steel Compos. Struct.*, **25**(6), 693-704.

Ahmed, A. (2014), "Post buckling analysis of sandwich beams with functionally graded faces using a consistent higher order theory", *Int. J. Civ. Struct. Environ.*, **4**(2), 59-64.

Ait Yahia, S., Ait Atmane, H., Houari, M.S.A. and Tounsi, A. (2015), "Wave propagation in functionally graded plates with porosities using various higher-order shear deformation plate theories", *Struct. Eng. Mech.*, **53**(6), 1143-1165.

Akbarzadeh, A.H., Abedini, A. and Chen, Z.T. (2015), "Effect of micromechanical models on structural responses of functionally graded plates", *Compos. Struct.*, **119**, 598-609.

Al-Basyouni, K.S., Tounsi, A. and Mahmoud, S.R. (2015), "Size dependent bending and vibration analysis of functionally graded micro beams based on modified couple stress theory and neutral surface position", *Compos. Struct.*, **125**, 621-630.

Attia, A., Bousahla, A.A., Tounsi, A., Mahmoud, S.R. and Alwabli, A.S. (2018), "A refined four variable plate theory for thermoelastic analysis of FGM plates resting on variable elastic foundations", *Struct. Eng. Mech.*, **65**(4). 453-464.

Barati, M.R. and Shahverdi, H. (2016), "A four-variable plate theory for thermal vibration of embedded FG nanoplates under non-uniform temperature distributions with different boundary conditions", *Struct. Eng. Mech.*, **60**(4), 707-727.

Behravan Rad, A. (2015), "Thermo-elastic analysis of functionally graded circular plates resting on a gradient hybrid foundation", *Appl. Math. Comput.*, **256**, 276-298.

Behravan, R. (2012), "Static response of 2-D functionally graded circular plate with gradient thickness and elastic foundations to compound loads", *Struct. Eng. Mech.*, **44**(2), 139-161.

Belabed, Z., Bousahla, A.A., Houari, M.S.A., Tounsi, A. and Mahmoud, S.R. (2018), "A new 3-unknown hyperbolic shear deformation theory for vibration of functionally graded sandwich plate", *Earthq. Struct.*, **14**(2), 103-115.

Belabed, Z., Houari, M.S.A., Tounsi, A., Mahmoud, S.R. and Anwar Bég, O. (2014), "An efficient and simple higher order shear and normal deformation theory for functionally graded material (FGM) plates", *Compos. Part B Eng.*, **60**, 274-283.

Bellifa, H., Bakora, A., Tounsi, A., Bousahla, A.A. and Mahmoud, S.R. (2017a), "An efficient and simple four variable refined plate theory for buckling analysis of functionally graded plates", *Steel Compos. Struct.*, **25**(3), 257-270.

Bellifa, H., Benrahou, K.H., Bousahla, A.A., Tounsi, A. and Mahmoud, S.R. (2017b), "A nonlocal zeroth-order shear deformation theory for nonlinear postbuckling of nanobeams", *Struct. Eng. Mech.*, **62**(6), 695-702.

Bennai, R., Ait Atmane, H. and Tounsi, A. (2015), "A new higher order shear and normal deformation theory for functionally graded sandwich beams", *Steel Compos. Struct.*, **19**(3), 521-546.

Bennoun, M., Houari, M.S.A. and Tounsi, A. (2016), "A novel five variable refined plate theory for vibration analysis of functionally graded sandwich plates", *Mech. Adv. Mater. Struct.*, **23**(4), 423-431.

Benyoucef, S., Mechab, I., Tounsi, A., Fekrar, A., Ait Atmane, H. and Adda Bedia, E.A. (2010), "Bending of thick functionally graded plates resting on Winkler-Pasternak elastic foundations", *Mech. Compos. Mater.*, **46**(4), 425-434.

Bouafia, K., Kaci, A., Houari, M.S.A., Benzair, A. and Tounsi, A. (2017), "A nonlocal quasi-3D theory for bending and free flexural vibration behaviors of functionally graded nanobeams", *Smart Struct. Syst.*, **19**(2), 115-126.

Bouderba, B., Houari, M.S.A. and Tounsi, A. (2013), "Thermomechanical bending response of FGM thick plates resting on Winkler-Pasternak elastic foundations", *Steel Compos. Struct.*, **14**(1), 85-104.

Bouderba, B., Houari, M.S.A., Tounsi, A. and Mahmoud, S.R. (2016), "Thermal stability of functionally graded sandwich plates using a simple shear deformation theory", *Struct. Eng. Mech.*, **58**(3), 397-422.

Bounouara, F., Benrahou, K.H., Belkorissat, I. and Tounsi, A. (2016), "A nonlocal zeroth-order shear deformation theory for free vibration of functionally graded nanoscale plates resting on elastic foundation", *Steel Compos. Struct.*, **20**(2), 227-249.

Bourada, M., Kaci, A., Houari, M.S.A. and Tounsi, A. (2015), "A new simple shear and normal deformations theory for functionally graded beams", *Steel Compos. Struct.*, **18**(2), 409-423.

Bousahla, A.A., Benyoucef, S., Tounsi, A. and Mahmoud, S.R. (2016), "On thermal stability of plates with functionally graded

coefficient of thermal expansion", *Struct. Eng. Mech.*, **60**(2), 313-335.

Bousahla, A.A., Houari, M.S.A., Tounsi, A. and Adda Bedia, E.A. (2014), "A novel higher order shear and normal deformation theory based on neutral surface position for bending analysis of advanced composite plates", *Int. J. Comput. Meth.*, **11**(6), 1350082.

Cho, J.R. and Ha, D.Y. (2001), "Averaging and finite-element discretization approaches in the numerical analysis of functionally graded materials", *Mater. Sci. Eng.*, **302**(2), 187-196.

Draiche, K., Tounsi, A. and Mahmoud, S.R. (2016), "A refined theory with stretching effect for the flexure analysis of laminated composite plates", *Geomech. Eng.*, **11**(5), 671-690.

El-Haina, F., Bakora, A., Bousahla, A.A., Tounsi, A. and Mahmoud, S.R. (2017), "A simple analytical approach for thermal buckling of thick functionally graded sandwich plates", *Struct. Eng. Mech.*, **63**(5), 585-595.

Feldman, E. and Aboudi, J. (1997), "Buckling analysis of functionally graded plates subjected to uniaxial loading", *Compos. Struct.*, **38**(1-4) , 29-36.

Ferreira, A.J.M., Batra, R.C., Roque, C.M.C., Qian, L.F. and Jorge, R.M.N. (2006), "Natural frequencies of functionally graded plates by a meshless method", *Compos. Struct.*, **75**(1-4), 593-600.

Ferreira, A.J.M., Batra, R.C., Roque, C.M.C., Qian, L.F. and Martins, P.A.L.S. (2005), "Static analysis of functionally graded plates third-order shear deformation theory and a meshless method", *Compos. Struct.*, **69**(4), 449-457.

Fourn, H., Ait Atmane, H., Bourada, M., Bousahla, A.A., Tounsi, A. and Mahmoud, S.R. (2018), "A novel four variable refined plate theory for wave propagation in functionally graded material plates", *Steel Compos. Struct.*, **27**(1), 109-122.

Gasik, M. and Lilius, R. (1994), "Evaluation of properties of W-Cu functional gradient materials by micromechanical model", *Comput. Mater. Sci.*, **3**(1), 41-49.

Gasik, M.M. (1998), "Micromechanical modeling of functionally graded materials", *Comput. Mater. Sci.*, **13**(1-3), 42-55.

Hamidi, A., Houari, M.S.A., Mahmoud, S.R. and Tounsi, A. (2015), "A sinusoidal plate theory with 5-unknowns and stretching effect for thermomechanical bending of functionally graded sandwich plates", *Steel Compos. Struct.*, **18**(1), 235-253.

Hashin, Z. and Shtrikman, S. (1963), "A variational approach to the theory of the elastic behaviour of multiphase materials", *J. Mech. Phys. Solids*, **11**(2),127-140.

Hazanov, S. (1998), "Hill condition and overall properties of composites", *Arch. Appl. Mech.*, **68**(6), 385-394.

Hebali, H., Tounsi, A., Houari, M.S.A., Bessaim, A. and Adda Bedia, E.A. (2014), "A new quasi-3D hyperbolic shear deformation theory for the static and free vibration analysis of functionally graded plates", *J. Eng. Mech.*, **140**(2), 374-383.

Hill, R. (1963), "Elastic properties of reinforced solids: Some theoretical principles", *J. Mech. Phys. Solids*, **11**(5), 357-372.

Kaci, A., Houari, M.S.A., Bousahla, A.A., Tounsi, A. and Mahmoud, S.R. (2018), "Post-buckling analysis of shear-deformable composite beams using a novel simple two-unknown beam theory", *Struct. Eng. Mech.*, **65**(5), 621-631.

Kant, T. and Khare, R.K. (1997), "A higher-order facet quadrilateral composite shell element", *Int. J. Numer. Meth. Eng.*, **40**, 4477-4499.

Kant, T. and Pandya, B. (1988), "A simple finite element formulation of a higher-order theory for unsymmetrically laminated composite plates", *Compos. Struct.*, **9**(3), 215-246.

Kar, V.R., Panda, S.K. and Mahapatra, T.R. (2016), "Thermal buckling behaviour of shear deformable functionally graded single/doubly curved shell panel with TD and TID properties", *Adv. Mater. Res.*, **5**(4), 205-221.

Karami, B., Shahsavari, D. and Janghorban, M. (2017), "Wave propagation analysis in functionally graded (FG) nanoplates under in-plane magnetic field based on nonlocal strain gradient theory and four variable refined plate theory", *Mech. Adv. Mater. Struct.*, **25**(12), 1047-1057.

Karami, B., Janghorban, M. and Li., L. (2018a), "On guided wave propagation in fully clamped porous functionally graded nanoplates", *Acta Astronaut.*, **143**, 380-390.

Karami, B., Shahsavari, D. and Li., L. (2018b), "Temperature-dependent flexural wave propagation in nanoplate-type porous heterogenous material subjected to in-plane magnetic field", *J. Therm. Stresses*, **41**(4), 483-499.

Karami, B., Shahsavari, D., Li., L., Karami, M. and Janghorban, M. (2018c), "Thermal buckling of embedded sandwich piezoelectric nanoplates with functionally graded core by a nonlocal second-order shear deformation theory", *Proc. Inst. Mech. Eng. Part C J. Mech. Eng. Sci.*, 0954406218756451.

Koizumi, M. (1993), "Concept of FGM", *Ceramic Tran.*, **34**, 3-10.

Koizumi, M. (1997), "FGM activities in Japan", *Compos. Part B Eng.*, **28**(1-2), 1-4.

Larbi Chaht, F., Kaci, A., Houari, M.S.A., Tounsi, A., Anwar Bég, O. and Mahmoud, S.R. (2015), "Bending and buckling analyses of functionally graded material (FGM) size-dependent nanoscale beams including the thickness stretching effect", *Steel Compos. Struct.*, **18**(2), 425-442.

Lo, K.H., Christensen, R.M. and Wu, E.M. (1977), "A high-order theory of plate deformation-Part 2: Laminated plates", *J. Appl. Mech.*, **44**, 669-674.

Mahdavian, M. (2009), "Buckling analysis of simply-supported functionally graded rectangular plates under non-uniform in-plane compressive loading", *J. Solid Mech.*, **1**, 213-225.

Meradjah, M., Kaci, A., Houari, M.S.A., Tounsi, A. and Mahmoud, S.R. (2015), "A new higher order shear and normal deformation theory for functionally graded beams", *Steel Compos. Struct.*, **18**(3), 793-809.

Mindlin, R.D. (1951), "Influence of rotary inertia and shear on flexural motions of isotropic, elastic plates", *J. Appl. Mech.*, **18**, 31-38.

Mohammadi, M., Saidi, A.R. and Jomehzadeh, E. (2010), "Levy solution for buckling analysis of functionally graded rectangular plates", *Appl. Compos. Mater.*, **17**(2), 81-93.

Mokhtar, Y., Heireche, H., Bousahla, A.A., Houari, M.S.A., Tounsi, A. and Mahmoud, S.R. (2018), "A novel shear deformation theory for buckling analysis of single layer graphene sheet based on nonlocal elasticity theory", *Smart Struct. Syst.*, **21**(4), 397-405.

Nelson, R.B. and Lorch, D.R. (1974) "A refined theory for laminated orthotropic plates", *J. Appl. Mech.*, **41**(1), 177-184.

Othman, M.I.A., Lotfy, K., Said, S.M. and Anwar Bég, O. (2012) "Wave propagation in a fiber-reinforced micropolar thermoelastic medium with voids using three models", *Int. J. Appl. Math. Mech.*, **8**(12), 52-69.

Paulino, G.H., Jin, Z.H. and Dodds Jr., R.H. (2003), *Comprehensive Structural Integrity, Volume 2: Fundamental Theories and Mechanisms of Failure*, Elsevier Science, 607-644.

Rad, A.B., Farzan-Rad, M.R. and Majd, K.M. (2017), "Static analysis of non-uniform heterogeneous circular plate with porous material resting on a gradient hybrid foundation involving friction force", *Struct. Eng. Mech.*, **64**(5), 591-610.

Reddy, J.N. (1984), "A simple higher-order theory for laminated composite plates", *J. Appl. Mech.*, **51**(4), 745-752.

Reissner, E. (1945), "Reflection on the theory of elastic plates", *J. Appl. Mech.*, **38**(11), 1453-1464.

Reiter, T. and Dvorak, G.J. (1997), "Micromechanical models for graded composite materials", *J. Mech. Phys. Solids*, **45**(8), 1281-1302.

Reiter, T. and Dvorak, G.J. (1998), "Micromechanical models for graded composite materials: II. Thermomechanical loading", *J. Mech. Phys. Solids*, **46**(9), 1655-1673.

Reuss, A. (1929), "Berechnung der fliessgrenze von mischkristallen auf grund der plastizitätsbedingung für einkristalle", *Z. Angew. Math. Mech.*, **9**(1) 49-58.

Schmauder, S. and Weber, U. (2001), "Modelling of functionally graded materials by numerical homogenization", *Arch. Appl. Mech.*, **71**(2-3), 183-193.

Shahsavari, D., Shahsavarib, M., Li, L. and Karami, B. (2018), "A novel quasi-3D hyperbolic theory for free vibration of FG plates with porosities resting on Winkler/Pasternak/Kerr foundation", *Aerosp. Sci. Technol.*, **72**, 134-149.

Shen, H.S. and Wang, Z.X. (2012), "Assessment of Voigt and Mori-Tanaka models for vibration analysis of functionally graded plates", *Compos. Struct.*, **94**(7), 2197-2208.

Swaminathan, K., Naveenkumar, D.T., Zenkour, A.M. and Carrera, E. (2015) "Stress, vibration and buckling analyses of FGM plates-A state-of-the-art review", *Compos. Struct.*, **120**, 10-31.

Talha, M. and Singh, B.N. (2010), "Static response and free vibration analysis of FGM plates using higher order shear deformation theory", *Appl. Math. Modell.*, **34**(12), 3991-4011.

Tounsi, A., Houari, M.S.A., Benyoucef, S. and Adda Bedia, E.A. (2013), "A refined trigonometric shear deformation theory for thermoelastic bending of functionally graded sandwich plates", *Aerosp. Sci. Technol.*, **24**(1), 209-220.

Touratier, M. (1991), "An efficient standard plate theory", *Int. J. Eng. Sci.*, **29**(8), 901-916.

Vel, S.S. and Batra, R.C. (2004), "Three-dimensional exact solution for the vibration of functionally graded rectangular plates", *J. Sound. Vib.*, **272**(3-5), 703-730.

Voigt, W. (1889), "Über die beziehung zwischen den beiden elastizitätskonstanten isotroper körper", *Wied. Ann. Phys.*, **38**(2), 573-587.

Wang, Y.Q. and Zu, J.W. (2017a), "Nonlinear steady-state responses of longitudinally traveling functionally graded material plates in contact with liquid", *Compos. Struct.*, **164**, 130-144.

Wang, Y.Q. and Zu, J.W. (2017b), "Nonlinear dynamic thermoelastic response of rectangular FGM plates with longitudinal velocity", *Compos. Part B Eng.*, **117**, 74-88.

Wang, Y.Q. and Zu, J.W. (2017c), "Analytical analysis for vibration of longitudinally moving plate submerged in infinite liquid domain", *Appl. Math. Mech.*, **38**(5), 625-646.

Yamanouchi, M., Koizumi, M., Hirai, T. and Shiota, I. (1990), *Proceedings of the 1st International Symposium on Functionally Gradient Material*, Sendai, Japan, October.

Yazid, M., Heireche, H., Tounsi, A., Bousahla, A.A. and Houari, M.S.A. (2018), "A novel nonlocal refined plate theory for stability response of orthotropic single-layer graphene sheet resting on elastic medium", *Smart Struct. Syst.*, **21**(1), 15-25.

Yin, H.M., Sun, L.Z. and Paulinho, G.H. (2004), "Micromechanics-based elastic model for functionally graded materials with particle interactions", *Acta Mater.*, **52**(12), 3535-3543.

Youcef, D.O., Kaci, A., Benzair, A., Bousahla, A.A., Tounsi, A. (2018), "Dynamic analysis of nanoscale beams including surface stress effects", *Smart Struct. Syst.*, **21**(1), 65-74.

Younsi, A., Tounsi, A, Zaoui, F.Z., Bousahla, A.A. and Mahmoud, S.R. (2018), "Novel quasi-3D and 2D shear deformation theories for bending and free vibration analysis of FGM plates", *Geomech. Eng.*, **14**(6), 519-532.

Zemri, A., Houari, M.S.A., Bousahla, A.A. and Tounsi, A. (2015), "A mechanical response of functionally graded nanoscale beam: An assessment of a refined nonlocal shear deformation theory beam theory", *Struct. Eng. Mech.*, **54**(4), 693-710.

Zidi, M., Tounsi, A., Houari, M.S.A., Adda Bedia, E.A. and Anwar Bég, O. (2014), "Bending analysis of FGM plates under hygro-thermo-mechanical loading using a four variable refined plate theory", *Aerosp. Sci. Technol.*, **34**, 24-34.

Zine, A, Tounsi, A., Draiche, K., Sekkal, M. and Mahmoud, S.R. (2018), "A novel higher-order shear deformation theory for bending and free vibration analysis of isotropic and multilayered plates and shells", *Steel Compos. Struct.*, **26**(2), 125-137.

Zuiker, J.R. (1995) "Functionally graded materials: Choice of micromechanics model and limitations in property variation", *Compos. Eng.*, **5**(7), 807-819.

CC